Published in final edited form as:
Int J Biochem Cell Biol. 2011 August ; 43(8): 1228–1239. doi:10.1016/j.biocel.2011.04.016.

Structural Requirements for the Inhibition of Calcium Mobilization and Mast Cell Activation by the Pyrazole Derivative BTP2

Mankit Law[1,2,4], **J. Luis Morales**[1], **Laurie F. Mottram**[3], **Archana Iyer**[1,2,#], **Blake R. Peterson**[3,†], and **Avery August**[1,2,4,*]

[1]Center for Molecular Immunology and Infectious Disease, Department of Veterinary and Biomedical Sciences, The Pennsylvania State University, University Park, PA 16802, USA

[2]Huck Institutes of the Life Sciences, Immunology and Infectious Diseases Graduate Program, The Pennsylvania State University, University Park, PA 16802, USA

[3]Department of Chemistry, The Pennsylvania State University, University Park, PA 16802, USA

[4]Department of Microbiology & Immunology, Cornell University, Ithaca, NY, USA

Abstract

Mast cells play a critical role in the development of the allergic response. Upon activation by allergens and IgE via the high affinity receptor for IgE (FcεRI), these cells release histamine and other functional mediators that initiate and propagate immediate hypersensitivity reactions. Mast cells also secrete cytokines that can regulate immune activity. These processes are controlled, in whole or part, by increases in intracellular Ca^{2+} induced by the FcεRI. We show here that N-(4-(3,5-bis(Trifluoromethyl)-1H-pyrazol-1-yl)phenyl)-4-methyl-1,2,3-thiadiazole-5-carboxamide (BTP2), a pyrazole derivative, inhibits activation-induced Ca^{2+} influx in the rat basophil cell line RBL-2H3 and in bone marrow-derived mast cells (BMMCs), without affecting global tyrosine phosphorylation of cellular proteins or phosphorylation of the mitogen-activated protein kinases Erk1/2 and p38. BTP2 also inhibits activation-induced degranulation and secretion of Interleukin (IL)-2, IL-3, IL-4, IL-6, IL-13, Tumor Necrosis Factor (TNF)-α, and Granulocyte Macrophage-Colony Stimulating Factor (GM-CSF) by BMMCs, which correlates with the inhibition of Nuclear Factor of Activated T cells (NFAT) translocation. *In vivo*, BTP2 inhibits antigen-induced

*Correspondence at current address: Avery August, Department of Microbiology & Immunology, College of Veterinary Medicine, VMC 5117, Cornell University, Ithaca, NY, 14853-6401, USA. (607) 253-3401 (Ofc), (607) 253-4058 (Fax), averyaugust@cornell.edu.
#Present Address: Joint Centers for Systems Biology, Columbia University, 1130 St. Nicholas Avenue, New York, NY 10032, USA.
†Present Address: Department of Medicinal Chemistry, University of Kansas, 1251 Wescoe Hall Drive, 4070 Malott Hall, Lawrence, Kansas 66045-7582, USA

[1]**Abbreviations:** AP-1, Activator Protein-1; BTP2, N-(4-(3,5-bis(Trifluoromethyl)-1H-pyrazol-1-yl)phenyl)-4-methyl-1,2,3-thiadiazole-5-carboxamide; $[Ca^{2+}]_i$, intracellular calcium concentration; CRAC channel, Calcium Release-Activated Calcium Channel; FcεRI, High affinity receptor for Fc portion of IgE; GATA1, GATA binding factor 1; GATA2, GATA binding factor 2; MAPK, Mitogen-Activated Protein Kinase; Erk1/2, Extracellular signal-regulated kinase 1/2; RBL, Rat Basophil Leukemia; RF, relative Fluorescence; SAPK/JNK, Stress-Activated Protein Kinase/c-Jun N-terminal Kinase;, Sp-1, Specificity Protein 1; STIM1, Stromal interaction molecule 1; NFATc1, Nuclear Factor of Activated T-cells cytoplasmic 1; TRPC, Transient receptor potential channel.

There are no conflicts of interests to report.

histamine release. Structure-activity relationship analysis indicates that substitution at the C3 or C5 position of the pyrazole moiety on BTP2 (5-triflouromethyl-3-methyl-pyrazole or 3-triflouromethyl-5-methyl-pyrazole, respectively) affected its activity, with the trifluoromethyl group at the C3 position being critical to its activity. We conclude that BTP2 and related compounds may be potent modulators of mast cell responses and potentially useful for the treatment of symptoms of allergic inflammation.

1. Introduction

Mast cells are integral members of the immune system. They are implicated in host responses to pathogens, autoimmune diseases, fibrosis, and wound healing. In addition, mast cells are the central effector cells in pathogenesis of allergic diseases, including anaphylaxis and allergic asthma. This is due, in large part, to the interaction between IgE and its receptor on mast cells, the FcεRI. Aggregation of FcεRI by polyvalent allergen recognized by bound IgE activates mast cells, subsequently initiating an immediate hypersensitivity reaction, as well as a late-phase reaction. The immediate reaction includes degranulation of preformed mediators and the release of rapidly synthesized lipid mediators. These mediators contribute to many allergic symptoms, ranging from erythema and edema to bronchospasm and mucous secretion in the lower respiratory tract. Late-phase reactions occur 6 to 24 hours after the immediate reaction and are mediated by cytokines and chemokines. The effects of these reactions include edema and leukocytic influx which contribute to persistent asthma (Stone et al., 2010).

FcεRI-triggered biphasic increase in cytosolic calcium (Ca^{2+}) is an essential step during mast cell activation and in the generation of productive mast cell responses, particularly degranulation. The FcεRI is triggered by IgE and antigen aggregation, which initiates several signaling pathways, activating phospholipase Cγ (PLCγ). PLCγ cleaves phosphatidylinositol 4,5-bisphosphate and generates the secondary messengers inositol triphosphate (IP_3) and diacylglycerol. Thereafter, a very small, transient cytosolic Ca^{2+} rise via Ca^{2+} efflux from IP_3-sensitive intracellular Ca^{2+} stores and a subsequent sustained Ca^{2+} influx across the plasma membrane through CRAC channels is produced, and Ca^{2+}-dependent transcription factors are activated (Feske, 2007, Gwack et al., 2007, Ishikawa et al., 2003b). The close correlation between Ca^{2+} mobilization, especially in the form of store-operated Ca^{2+} entry, and gene expression of chemokines and cytokines underscores the importance of cytosolic Ca^{2+} increases for mast cell function. Moreover, Ca^{2+} mobilization is central for driving the degranulation of histamine-containing vesicles and *de novo* synthesis of lipid mediators (Di Capite and Parekh, 2009, Scharenberg and Kinet, 1998, Turner and Kinet, 1999). In fact, mice lacking the CRAC channel components Orai1 or STIM1, exhibit severely impaired histamine release and leukotriene production, reduced TNF-α secretion, and an inability to mount a subcutaneous anaphylactic response (Baba et al., 2008, Vig et al., 2008).

Specific inhibitors of the Ca^{2+} signaling pathway are potential therapeutics for various immune and allergic diseases. As experimental tools, they could also facilitate molecular identification of mechanisms of Ca^{2+} mobilization, particularly those governing CRAC channel gating. Unfortunately, blockers, such as SK&F 96365, econazole, and 2-aminoethyldiphenylborate, have IC_{50} values in the micromolar range and are non-specific (Braun et al., 2003, Chung et al., 1994, Franzius et al., 1994, Ma et al., 2002, Peppiatt et al., 2003, Prakriya and Lewis, 2001, Schindl et al., 2002, Wu et al., 2000, Zitt et al., 2004).

A number of groups have defined pyrazole derivatives exemplified by BTP2, that specifically block T-cell receptor (TCR)-induced Ca^{2+} entry and Ca^{2+}-dependent cytokine

production (Djuric et al., 2000, Trevillyan et al., 2001, Ishikawa et al., 2003a, Mercer et al., Zitt et al., 2004, Mercer et al., 2010). As mast cell activation and degranulation is critically dependent on increases in intracellular Ca^{2+}, compounds that inhibit this process would be useful as potential therapeutics for allergies and asthma. However, limited work has been done to further characterize the structural requirements for the pharmacological efficacy of these pyrazole-derived compounds, such as BTP2 (Di Capite and Parekh, 2009). Here, we have investigated the effect of BTP2 on activation of RBL-2H3 cells and bone marrow-derived mast cells (BMMC), as well as *in vivo* in a murine system to evaluate the therapeutic potential of this compound for the treatment of mast cell-exacerbated diseases. Additionally, we provide a structure-activity relationship analysis of derivatives of the BTP, defining the active portion of the BTP2 parent compound.

2. Experimental Procedures

2.1. Cell Culture and Reagents

RBL-2H3 cells (American Type Culture Collection, Manassas, VA, USA) were cultured at 37°C in Dulbecco's Modified Eagle Medium (DMEM) supplemented with 15% heat-inactivated fetal bovine serum (FBS), 100 U/mL penicillin, 100 μg/mL streptomycin, and 1% minimal essential medium non-essential amino acid solution. Mouse BMMCs were grown from femoral marrow cells of C57BL/6 mice as previously described with a few changes (Iyer and August, 2008). In brief, bone marrow cells were obtained from 6–10-week-old mice and cultured in DMEM, supplemented with 10% FBS, 100 U/mL penicillin, 100 μg/mL streptomycin, 100 μM nonessential amino acids, 1 mM sodium pyruvate, 1 mM glutamine, 50 μM 2-β-mercaptoethanol (2-ME), IL-3 (10 ng/mL), and Stem Cell Factor (SCF, 50 ng/mL). Cells were passaged every two days by replating the cells in fresh medium. BMMCs were used for experiments after 4–8 weeks of culture (>95% mast cells) and were routinely >95% positive for cell surface expression of FcεRI and c-kit. BTP2 (YM-58483; N-(4-(3,5-bis(Trifluoromethyl)-1H-pyrazol-1-yl)phenyl)-4-methyl-1,2,3-thiadiazole-5-carboxamide) was purchased from Calbiochem while other derivatives were synthesized as previously described (Djuric et al., 2000; Mercer et al., 2010b). Both 2-Aminoethoxydiphenyl borate (2-APB) and ≥99.9% anhydrous dimethyl sulfoxide (DMSO) were purchased from Sigma-Aldrich. For all experiments, DMSO was utilized for vehicle control purposes at a maximum concentration of 1 μL/mL (~14 μM or 1:1000 dilution).

2.2. Measurements of Intracellular Calcium

$[Ca^{2+}]_i$ was measured using the Ca^{2+}-reactive fluorescent probe Fura-2 acetoxymethylester (Fura-2AM) as previously described (Iyer and August, 2008). First, cells were pretreated with 1 μM BTP2 or vehicle for 1 hr at 37°C and, thereafter, washed with Ringer's Solution (155 mM NaCl, 4.5 mM KCl, 2 mM $MgCl_2$, 10 mM dextrose, 5 mM HEPES, pH 7.4), supplemented with 1 mM $CaCl_2$. Cells were loaded with 1 μM Fura-2AM at a concentration of 10^7 cells/mL in Ca^{2+}-supplemented Ringer's Solution for 1 hr in the dark. Cells were then washed, resuspended in Ca^{2+} supplemented Ringer's Solution, and the $[Ca^{2+}]_i$ of 5×10^5 cells was monitored using a Photon Technology International Quantamaster Spectrofluorometer. Fluorescence of Fura-2AM was monitored at room temperature. $[Ca^{2+}]_i$ was expressed as the ratio (Relative Fluorescence, RF) of Fura-2AM fluorescence at 510 nM caused by the two excitation wavelengths (340 nm/380 nm). $[Ca^{2+}]_i$ in BMMCs was measured using the Ca^{2+} indicator Fluo-4 (Molecular Probes). BMMCs were sensitized with mouse IgE anti-dinitrophenyl (DNP) at a concentration of 1 μg IgE anti-DNP/2×10^6 cells/mL in medium starved of IL-3 and SCF overnight, washed, and resuspended in factor-starved media. Then, the cells were treated with BTP2 (1 μM), 3T5M-P, or vehicle for 1 hr at 37°C and loaded with Fluo-4 according to manufacturer's instructions. Subsequently, the cell suspension was supplemented with 2 mM $CaCl_2$. The $[Ca^{2+}]_i$ of 1.25×10^6 cells was

monitored using a FC500 Benchtop Cytometer. RF of Fluo-4 was measured at 494 nm when excited by 488 nm of light at room temperature. $[Ca^{2+}]_i$ was expressed as the RF of Fluo-4. Mean calcium post-stimulation was calculated as the mean of $[Ca^{2+}]_i$ ratiometric Fura-2AM or Fluo-4 RF measurements post-stimulation after subtracting the mean of baseline measurements pre-treatment. Peak calcium post-stimulation was calculated as the maximum $[Ca^{2+}]_i$ ratiometric Fura-2AM or Fluo-4 RF measurement post-stimulation after subtracting the mean of respective pre-treatment baseline measurements.

2.3. Western Blotting

BMMCs were sensitized with 1 μg mouse IgE anti-DNP/mL overnight, incubated with 1 μM BTP2 or vehicle for 30 min at 37°C, washed with phosphate-buffered saline (PBS) solution once, and finally challenged with 100 ng DNP-human serum albumin (HSA)/mL for indicated times (0–60 min). After challenge, the cells were lysed in RIPA lysis buffer supplemented with phosphatase inhibitors on ice. To quantitate the protein concentration of whole cell lysates, the bicinchoninic acid (BCA) protein assay (Pierce Biotechnology, Rockford, IL) was performed. Subsequently, polyacrylamide gels were loaded with 20–25 μg protein per well (depending upon the experiment), and SDS-PAGE and western blotting were performed as previously described (Iyer and August, 2008). Blots were probed with the following antibodies: anti-phospho-Erk1/2 (Thr^{202}, Tyr^{204}), anti-phospho-SAPK/JNK (Thr^{183}, Tyr^{185}), anti-phospho-p38 (Thr^{180}, Tyr^{182}), and anti-c-fos (all from Cell Signaling Technology, Beverly, MA), followed by horseradish peroxidase (HRP)-linked goat anti-mouse or goat anti-rabbit Ig. HRP-linked anti-phospho-tyrosine was also used. Blots were stripped and reprobed with anti-β-actin control antibodies. Blots were developed in chemiluminescent reagents and exposed to x-ray film. Densitometric analysis of the western blots was performed with ImageJ software, and the data was standardized to the level of β-actin.

2.4. Cytokine Secretion Assay

Analysis of cytokine secretion by BMMCs were performed as previously described (Iyer and August, 2008), except that cells were also incubated in the presence of 1 μM BTP2 or vehicle for 30 min on ice in Tyrode's buffer prior to stimulation. In brief, cells were washed and sensitized with or without mouse IgE anti-DNP (1 μg/mL) in the absence of IL-3 or SCF overnight to remove exogenous IL-3. Thereafter, the cells were washed and resuspended in Tyrode's buffer. Cells were then incubated in the presence of 1 μM BTP2 or vehicle for 30 min on ice in Tyrode's buffer and, afterwards, stimulated in medium starved of IL-3 and SCF in V-bottom 96-well culture plates (2×10^5 cells/150 μL). Cells were stimulated with 50 nM phorbol myristic acid (PMA) and 500 nM ionomycin in the presence or absence of 1 μM BTP2. Alternatively, cells were stimulated with 15 μg rat anti-mouse IgE/mL or 100 ng DNP-HSA/mL in the presence of absence of 1 μM BTP2. Cytokines in cell culture supernatants obtained 8 h and 24 h after stimulation was measured using a Milliplex MAP immunoassay according to the suppliers' instructions. Within the assay sensitivities, mouse interleukin (IL)-2, IL-3, IL-4, IL-6, IL-13, tumor necrosis factor (TNF-α), and granulocyte-macrophage colony-stimulating factor (GM-CSF) were detected. IL-17 and IFN-γ were not detected. Cytokine concentrations are reported in pg/mL units.

2.5. Analysis of NFAT Localization

RBL-2H3 cells were cultured in glass bottom 6-well plates (2×10^5 cells/2 mL) overnight. For DNP-HSA stimulation, cells were sensitized with 1 μg mouse IgE anti-DNP/mL overnight, washed, and resuspended in factor-starved media. Then, the cells were treated with 1 μM BTP2 or vehicle for 30 min at 37°C, stimulated with 50 nM PMA and 500 nM ionomycin or 100 ng/mL DNP-HSA for 45 min at 37°C, and washed with PBS once. The cells were immediately fixed and permeabilized in a 50:50 methanol:acetone mixture for, at

least, 15 min at −20°C. The cells were subsequently washed with PBS three times, blocked with normal rat serum for 2 h at room temperature, and stained with Alexa Fluor 488-conjugated mouse IgG anti-Nuclear Factor of Activated T-cells, cytoplasmic 1 (NFATc1) (Santa Cruz Biotechnology, Inc.) overnight at 4°C. Then, the cells were stained with TO-PRO-3 for identification of localization of the nucleus. After staining, cells were observed using an Olympus Fluoview 1000 confocal microscope for fluorescence at 519 nm with an excitation wavelength of 488 nm. At a 100× magnification, images were captured at 0.2 μm slices as Z-plane stacks. Data was analyzed with Autodeblur and Autovisualize X licensed software for deconvolution and 3-D image processing.

2.6. Quantitative Real-Time PCR Analysis

BMMCs (5×10^6 cells) were treated with 1 μM BTP2 or vehicle and cultured for 2 days. Total RNA was prepared from the treated populations, using a RNeasy Mini Kit (Qiagen Sciences, MD). Complementary DNA (cDNA) was generated using Ready-To-Go You-Prime First-Strand Beads (GE Healthcare, Buckinghamshire, UK) per manufacturer's protocol. Quantitative PCR was performed with the ABI 7300 Real-Time PCR System using Taqman gene expression assay probes for IL-4, IL-6, and TNF-α, with glyceraldehyde 3-phosphate dehydrogenase (GAPDH) as a housekeeping gene (Applied Biosystems, Branchburg, NJ). Data was analyzed using the Comparative $\Delta\Delta C_T$ (threshold cycle) method. Expression of IL-4, IL-6, and TNF-α was normalized based on the levels of mRNA for GAPDH and set relative to a calibrator sample. The normalized relative gene expression levels of samples were then compared with the expression level of vehicle-treated populations, set as 1.

2.6. Degranulation Assays

RBL-2H3 cells were seeded at 2×10^5 per well (in 1 mL) of a 12-well cell culture plate and cultured overnight. In some cases, the cells were treated with BTP2, 2-APB (at 50 μM), BTP2 derivatives (at the indicated concentrations or 1 μM), or vehicle for 30 min at 37°C and subsequently challenged with 500 nM ionomycin for 30 min at 37°C. Alternatively, the cells were sensitized with 1 μg mouse IgE anti-ovalbumin (OVA)/mL for 3 hr at 37°C. The cells were washed with PBS, treated with BTP2, BTP2 derivatives, or vehicle for 30 min at 37°C, and then treated with 10 μg rat anti-mouse IgE in a final volume of 1 mL medium, supplemented with BTP2, BTP2 derivatives, or vehicle for 30 min at 37°C. Mast cell degranulation was quantitatively measured using a flow cytometric annexin-V binding assay (Demo et al., 1999). After stimulus, RBL-2H3 cells were washed with pre-chilled PBS twice and subsequently stained with annexin-V-phycoerythrin (PE) at a dilution of 1:20 in binding buffer (commercially available as a part of the annexin-V-PE (BD Pharmingen) for 15 min at room temperature. The cells were analyzed using a FC500 Benchtop Cytometer. Degranulation was calculated as a percentage of the mean fluorescence intensity (MFI) of PE fluorescence of live RBL-2H3 cells, challenged in the presence of negative control (vehicle) medium, after subtracting background release (% degranulation).

Degranulation was also determined by measuring the levels of secreted β-hexosaminidase. RBL-2H3 cells or BMMCs were treated as described above, except that after activation, β-hexosaminidase activity in the supernatants was determined spectrophotometrically. In brief, 50 μL of supernatant samples and 80 μL of pnitrophenyl-N-acetyl-β-D-glucosamide (pNAG) solubilized in 0.05 M citrate buffer (pH 4.5) were added to the wells of a flat-bottom 96-well plate. Color was allowed to develop for 30 min at 37°C. The enzymatic reaction was terminated with the addition of 200 μL 0.05 M sodium carbonate buffer (pH 10.0). Absorbances at 415 nm were measured in a microplate reader. Cells were lysed with 1% Triton-X, and the extracts were analyzed for endogenous β-hexosaminidase activity (total − test). The β-hexosaminidase activity in unstimulated cells (spontaneous) was

subtracted from the enzyme activity of the stimulated cells (test). The percentage of β-hexosaminidase released into each supernatant (% of total) was calculated using the following formula: β-hexosaminidase secretion (% of total) = (test − spontaneous)/(total − spontaneous) × 100. Degranulation was calculated as a percentage of the percentage released into each supernatant of total β-hexosaminidase (% of total) for BMMCs, challenged in the presence of negative control (vehicle) medium, after subtracting background release (% degranulation).

2.8. In Vivo Histamine Release Assay

Analysis of *in vivo* histamine release was determined as previously described (Iyer and August, 2008). In brief, C57BL/6 mice (n=3 per group, 8 weeks old) were sensitized with 1 μg of mouse IgE anti-DNP via intraperitoneal injection overnight. Twelve hours post-sensitization, mice were treated with 10 mg BTP2/kg (~50 μL in PBS per mouse) or vehicle (DMSO, 50 μL in PBS) as appropriate via intraperitoneal (i.p.) injection. One hour post treatment, mice were challenged with 50 μg DNP-HSA (solubilized in 100 μL PBS), which was delivered via intravenous injection Control mice were sensitized with mouse IgE anti-DNP, treated with DMSO or BTP2, and were challenged with PBS alone (i.e. no antigen). 3 min post-challenge, blood was collected by cardiac puncture and stored at 4°C until centrifugation was performed for the preparation of serum samples. Histamine was determined using a Beckman Coulter EIA Histamine Assay. All experiments were carried out in accordance with the regulations of IUCAC at The Pennsylvania State University.

2.9. Statistical Analysis

Data represent the mean ± standard error mean (SEM) of three independent experiments. The concentration causing 50% inhibition (IC_{50}) was calculated using non-linear regression analysis. The statistical significance was analyzed by Student's *t*-test (unpaired t-test, two-tailed) or by two-way ANOVA. Values of $p<0.05$ were considered significant. All data analyses were performed using FlowJo or GraphPad Prism 5.

3. Results

3.1. Effects of BTP2 on FcεRI-mediated signaling in RBL-2H3 cells and BMMCs

Increases in $[Ca^{2+}]_i$, triggered through the FcεRI by IgE and allergen are necessary for the functional responses of mast cells. To analyze the possibility that BTP2 has the potential to inhibit Ca^{2+} mobilization in mast cells, Ca^{2+} signals in the presence or absence of BTP2 were compared. We first used RBL-2H3 cells which have been used extensively as a mast cell model to study FcεRI signaling. These cells were pre-treated with BTP2 (1 μM) or vehicle (DMSO) for 30 min and, then, analyzed for calcium responses, as described in the materials and methods, following stimulation. These initial studies with RBL-2H3 cells involved stimulation with the established Ca^{2+} ionophore ionomycin, which can activate mast cell degranulation, as well as cytokine secretion, downstream (in the presence of the phorbol ester PMA) of the FcεRI (Gomperts et al., 1980, Gertler and Pecht, 1988, Plaut et al., 1989). We found that BTP2, at a 1 μM concentration, significantly reduced intracellular Ca^{2+} following stimulation by ionomycin (Fig. 1). Moreover, analysis of peak Ca^{2+} responses showed a significant difference in this parameter (Fig. 1*B*). Because ionomycin is not a physiological stimulus, we next tested whether Ca^{2+} responses following more physiological stimuli via the FcεRI were also inhibited by BTP2. In these experiments, we used anti-IgE, as well as the antigen specific IgE anti-DNP along with DNP-HSA, for activation of primary sensitized bone marrow-derived mast cells (BMMCs). These BMMCs were pre-treated with BTP2 (1 μM) or vehicle for 30 min, then stimulated with mouse anti-DNP IgE and rat anti-mouse IgE or antigen DNP-HSA for the indicated time period in the presence of $CaCl_2$. Data summarized in Fig. 1*A* and *C* reveal that BTP2 inhibited the Ca^{2+}

response in these BMMCs following FcεRI aggregation, with the Ca^{2+} peak significantly inhibited regardless of stimulation method (Fig. 1*B–C*).

By contrast, BTP2 did not affect FcεRI-triggered tyrosine phosphorylation of cellular proteins in BMMCs (Fig. 2*A*). Activation of Erk, JNK, and p38 MAPK pathways were also not affected by BTP2 treatment (Fig. 2, *B–D*, **respectively**). Finally, expression of c-Fos, which is dependent upon activation of Erk, was not altered by BTP2 treatment (Fig. 2*E*). Thus, BTP2 does not grossly affect phosphorylation events immediately downstream of the FcεRI.

3.2. BTP2 inhibits degranulation in RBL-2H3 cells

Mast cell degranulation is a highly regulated Ca^{2+}-dependent process (Melicoff et al., 2009). As BTP2 inhibits Ca^{2+} mobilization in RBL-2H3 cells and BMMCs (Fig. 1, *A–B*), we next determined if mast cell degranulation could be inhibited by BTP2. For these experiments, we used an annexin-V binding assay, as described in the materials and methods section. RBL-2H3 cells were pretreated with BTP2 or vehicle, at a 1 μM concentration, and then stimulated with ionomycin for 30 minutes, followed by analysis of degranulation. We found that BTP2 significantly reduced ionomycin-induced degranulation (Fig. 3*A*). This inhibition occurred in a dose-dependent fashion, with an IC_{50} value of 23 nM (Fig. 3*B*). Comparative analysis of population-based measurements of the secretion of the granule-derived enzyme β-hexosaminidase between BTP-treated cells and those that were treated with vehicle alone revealed inhibition of ionomycin-induced degranulation upon pre-treatment with BTP2, thereby validating the results generated through the annexin-V binding assay (Supplemental Fig. 1). Furthermore, BTP2 could also significantly reduce degranulation induced by FcεRI crosslinking with anti-IgE antibodies. In these experiments, RBL-2H3 cells were sensitized with mouse IgE anti-OVA, pretreated with vehicle or BTP2 (1 μM) for 30 minutes, and finally stimulated with rat anti-mouse IgE for 30 minutes. Our results indicate that BTP2 significantly reduced degranulation induced by FcεRI as well (Fig. 3*C*). BTP2 is therefore an effective inhibitor of mast cell degranulation induced through the FcεRI.

3.3. BTP2 inhibits histamine release in mice in response to antigenic challenge

To further characterize the effects of BTP2 on the mast cell-dependent physiological response of degranulation, we analyzed the effect of BTP2 on histamine release *in vivo*. Mice were sensitized with mouse IgE anti-DNP (1 μg) twelve hours prior to being pre-treated with 10 mg BTP2/kg or vehicle that was delivered intraperitoneally. These mice were then challenged with DNP-HSA an hour later to stimulate mast cell degranulation. Three minutes post-challenge with DNP-HSA, mice were sacrificed and serum collected and assayed for histamine. Control mice were exposed to anti-DNP IgE, but they were left unexposed to antigen to ensure that the measured responses were antigen-specific. The results show that BTP2 significantly reduces histamine release upon antigenic stimulation *in vivo* (Fig. 3*D*). In summary, this data provides strong support for the idea that BTP2 is a potent inhibitor of mast cell degranulation *in vivo*.

3.4. BTP2 inhibits NFAT nuclear localization and cytokine secretion in mast cells

BTP2 was originally reported to inhibit IL-2 production in activated Jurkat T-cells and human $CD4^+$ T-cells, as well as IL-4 and IL-5 production in antigen-stimulated murine Th2 clone D10.G4.1 cells (Djuric et al., 2000, Ishikawa et al., 2003a, Trevillyan et al., 2001, Zitt et al., 2004, Yoshino et al., 2007). BTP2 also inhibits NFAT activation in Jurkat T-cells and primary human T-cells (Djuric et al., 2000, Ishikawa et al., 2003a, Trevillyan et al., 2001, Zitt et al., 2004). Because secretion of these cytokines is regulated differently in mast cells in certain cases (Monticelli et al., 2005, Monticelli et al., 2004, Solymar et al., 2002, Bert et al., 2007), we tested whether the cytokine secretion of BMMCs is affected by BTP2.

BMMCs were stimulated with PMA and ionomycin in the presence or absence of BTP2, and supernatants were analyzed for IL-2, IL-3, IL-4, IL-13, TNF-α, and GM-CSF. As illustrated in Fig. 4, at both 8 and 24 hours after stimulation, BTP2 inhibited the secretion of IL-2, IL-3, IL-4 and TNF-α from BMMCs. While little IL-13 was detected at the 8 hour time point, BTP2 inhibited IL-13 secretion by BMMCs at the 24 hour time point (Fig. 4). By contrast, BTP2 significantly inhibited ionomycin-induced secretion of GM-CSF at the 24 h time point (Fig. 4).

We also analyzed cytokine secretion in sensitized BMMCs stimulated with anti-IgE. We found that there was little production of IL-2 and IL-13 up to 24 hours post-stimulation; however, BTP2 pre-treatment inhibited the secretion of IL-3, IL-4, IL-6, TNF-α, and GM-CSF (Fig. 5). Similar results were obtained for IL-4, IL-6 and TNF-α when sensitized BMMCs were stimulated with DNP-HSA (Fig. 6).

Because the cytokines that were inhibited by BTP2 are regulated, in part, by NFAT (Savignac et al., 2007, De Boer et al., 1999) and NFAT activation and nuclear translocation is dependent upon increases in cytosolic Ca^{2+}, we examined the effect of BTP2 on NFAT localization in stimulated RBL-2H3 cells. Cells were stimulated with ionomycin, and NFAT localization was examined. Alternatively, sensitized RBL-2H3 cells were stimulated with DNP-HSA. These experiments show that BTP2 inhibited ionomycin-induced, as well as antigen-IgE/FcεRI-induced, NFAT nuclear translocation (Fig. 7*A*, *B*).

We noted that BTP2 treatment completely suppressed the production of IL-2 and IL-3 but partially inhibited the secretion of IL-4, IL-6, and TNF-α (Fig. 4–6). To further elucidate the mechanism of inhibition responsible for this observation, we examined the effect of BTP2 on mRNA transcript levels for IL-4, IL-6 and TNF-α under steady state conditions in BMMCs. As illustrated in Fig. 8, BTP2 treatment did not significantly inhibit the levels of preformed mRNA transcripts for these cytokines suggesting that BTP2 inhibits cytokine production primarily via its effects upon *de novo* transcription that is regulated by NFAT or other Ca^{2+}-sensitive transcription factors during the late phase of mast cell activation through the IgE receptor.

3.5. The trifluoromethyl group at the C3 is required for the effect of BTP2

To determine which moiety within the BTP2 molecule is important for its activity, we performed limited structure-activity relationship studies of the BTP2 parent compound. We synthesized a series of BTP2 derivatives that have retained the core structure shared by all members of the BTP class of compounds but have been altered by replacing the electron-withdrawing trifluoromethyl groups of the BTP ring with less bulky electron-donating methyl groups (5T3M-P: 5-trifluoromethyl-3-methyl-pyrazole or 3T5M-P: 3-trifluoromethyl-5-methyl-pyrazole), deleting a single trifluoromethyl at either the C5 or C3 position (3T-P or 5TP), deleting the trifluoromethyl groups entirely (Pyrazole, Pyr), or replacing both trifluoromethyl groups with methyl groups (3M5M-P) (Fig. 9*A*). In addition, the remaining ring of BTP2 not shared by all members of the BTP class of compounds was replaced with the ring structure characteristic of BTP1 for these BTP2 derivatives (Kiyonaka et al., 2009) (Fig. 9*A*). Accordingly, BTP1 was also tested. The BTP2 parent compound and its derivatives (1 μM) were tested for their ability to inhibit degranulation in BMMCs upon ionomycin stimulation. BTP1 and BTP2 were indistinguishable in their ability to inhibit degranulation (Fig. 9*B*). In addition, Pyr did not suppress degranulation; however, 5T3M-P and 3T5M-P significantly reduced degranulation in comparison to vehicle-treated cells (Fig. 9*B*). However, 5T3M-P only inhibited degranulation by approximately 25%, whereas 3T5M-P was almost as potent as the parent BTP2 compound (Fig. 9*B*). Indeed, a derivative with only a single trifluoromethyl group at the C3 position (3T-P) was able to inhibit degranulation, while one with only a trifluoromethyl group at the C5 (5T-P) position was not

(Fig. 9*B*). Finally, replacing both trifluoromethyl groups with methyl groups (in 3M5M-P) gave similar results as complete lack of the trifluoromethyl groups (pyrazole) (Fig. 9*B*). The known calcium influx inhibitor 2-APB was used as a control demonstrating that this compound could also inhibit the response (Fig. 9*B*). 3T5M-P inhibited ionomycin-induced degranulation with an IC_{50} of 25 nM (Fig. 9*C*), and in line with this finding, 3T5M-P significantly inhibited DNP-HSA-IgE/FcεRI-induced calcium increases in BMMCs (Fig. 9*D*, *E*). These results suggest that the trifluoromethyl group at the C3 position of the pyrazole compound is critical for the inhibitory activity of BTP2 on degranulation.

4. Discussion

BTP2 has been characterized as a selective blocker of store-operated Ca^{2+} entry. We investigated the effect of BTP2 on mast cell function using the RBL-2H3 cell line and BMMCs *in vitro*, as well as in *in vivo* murine models, to evaluate its therapeutic potential in mast cell-mediated diseases. We show that BTP2 inhibits activation-induced increases in intracellular Ca^{2+} responses. In addition, we show that BTP2 inhibits IgE and antigen-induced degranulation *in vitro* and histamine release *in vivo*, as well as activation-induced cytokine secretion *in vitro*. Finally, we show that the 3-trifluoromethyl group on the pyrazole ring is critical for the activity of BTP.

Sustained intracellular Ca^{2+} increase is integral for allergen-induced mast cell activation. The activation of mast cells leads to the release of performed mediators that are stored in cytoplasmic granules. These mediators include histamine, serine proteases (tryptase and chymase), carboxypeptidase A, and proteoglycans (Stone et al.). The effects of BTP2 on mast cell degranulation and cytokine secretion *in vitro*, as well as histamine release *in vivo*, suggest that this compound could modulate the effect of histamine on smooth muscle contraction, endothelial cells function, nerve endings, and mucous secretion. This agrees with other studies suggesting that BTP2 may be efficacious in models of respiratory anaphylaxis in guinea pigs. In these models, BTP2 was able to inhibit increased bronchoconstriction and airway hyperresponsiveness (Ohga et al., 2008, Stone et al.).

Sustained elevations in $[Ca^{2+}]_i$ are also essential for the production and secretion of cytokines by mast cells, which can modulate subsequent immune responses (Di Capite and Parekh, 2009). The ability of BTP2 to inhibit cytokine secretion in BMMCs is likely due to reduced NFAT nuclear translocation since this transcription factor is essential for the expression of many cytokine genes in mast cells (Klein et al., 2006, Monticelli et al., 2004). Interestingly, BTP2 treatment completely suppressed ionomycin-induced, as well as FcεRI mediated, secretion of IL-2 and IL-3 but partially inhibited secretion of IL-4, IL-6 and TNF-α. In mast cells, TNF-α and IL-4 can be expressed from both preformed mRNA as well as newly transcribed mRNA (Gessner et al., 2005, Stone et al.). Indeed, BTP2 treatment did not affect the levels of preformed IL-4 and TNF-α mRNA. In addition, BTP2 also did not affect preformed levels of IL-6 mRNA. This suggests that translation of preformed mRNA for TNF-α and IL-4 in BMMCs is likely not affected by increases in $[Ca^{2+}]_i$. On the other hand, *de novo* transcription that is regulated by NFAT or other Ca^{2+}-sensitive transcription factors is likely affected by BTP2.

We also found that while BTP2 could significantly inhibit FcεRI-mediated GMCSF secretion, it was not as effective in inhibiting the secretion of this cytokine when the cells were stimulated with PMA and ionomycin, suggesting that this cytokine may be regulated differently and that its expression may not have as stringent a requirement for $[Ca^{2+}]_i$ increase. Indeed, analysis of the regulation of GM-CSF in transgenic mice has revealed multiple cis-acting elements that regulate this cytokine in T cells and mast cells (Bert et al., 2007). This analysis reveals that, in addition to NFAT, other transcription factors, such as

AP-1, Sp-1, GATA1, and GATA2 can be differentially used in different cell types to regulate GM-CSF expression (Bert et al., 2007). Thus, while both FcεRI- and PMA and ionomycin-mediated activation of mast cells result in GM-CSF secretion, they may act using slightly different combinations of transcription factors, with FcεRI activation being more calcium-dependent and thus more potently inhibited by BTP2.

Similar to the effects of BTP2 on WT BMMCs, BMMCs from mice lacking either Orai1 or STIM1 produce weak Ca^{2+} signals in response to agonist (Baba et al., 2008, Vig et al., 2008). These BMMCs are characterized by severely impaired histamine release, decreased leukotriene production, reduced TNF-α secretion, and a dysfunctional subcutaneous anaphylactic response. Therefore, Ca^{2+} entry through CRAC channels is essential for mast cell function (Baba et al., 2008, Di Capite and Parekh, 2009, Vig et al., 2008). Here, our profiling of the effects of BTP2 on mast cell activation and downstream responses suggests that BTP2 acts in a similar pathway. Our recent characterization of an interaction between BTP2 and the actin-regulating protein drebrin and the resultant discovery of a novel role for drebrin as a mediator of store-operated Ca^{2+} entry further implies such a mechanism of action (Mercer et al., 2010). Further analysis of the role of drebrin in calcium signaling and mast cell function will reveal insights into the mechanism behind this process.

We also explored the structure-activity relationship between BTP2 and mast cell degranulation. Our study indicates that the trifluoromethyl groups at positions C3 and C5 of the pyrazole compound play critical roles in the mechanism of action of the BTP2 parent compound, with the trifluoromethyl group at C3 being more critical for inhibitory activity of BTP2. While the 3T5M-P and 3T-P derivatives inhibited activation induced degranulation in BMMCs, the 5T3M-P, 5T-P, Pyr, and 3M5M-P derivatives were much less potent. These observed activities are similar to those reported by Kiyonaka et al. for pyrazole compounds that target the TRPC3 channel. This group recently showed that bulky functional groups at the 3,5-positions of the pyrazole may be important for the inhibition of Ca^{2+} mobilization via the TRPC3 channel (Kiyonaka et al., 2009). In this work, Kiyonaka et al. characterized the activity of a BTP derivative that substitutes the 3,5-bis(trifluoromethyl)pyrazole group with an ethyl-3-trifluoromethyl-pyrazole-4-carboxylate group in the BTP2 parent compound (4-(2,3,3-trichloroacrylamide)phenyl)-5-(trifluoromethyl)-1H-pyrazole-4-carboxylate). This compound selectively inhibited the TRPC3 channel and was a more potent inhibitor of NFAT in cardiac myocytes than BTP2. This work also showed that the 3,5-bis(trifluoromethyl)pyrazole group or a trichloroacrylic amide group is critical for the selectivity for TRPC5 or TRPC3, respectively (Kiyonaka et al., 2009). This suggests that the pyrazole group provides a molecular scaffold with which to develop inhibitors of calcium signaling (Kiyonaka et al., 2009). These analyses suggest that the attachment of bulky and/or electron-withdrawing groups on the pyrazole ring of such molecules, particularly in the C3 position is important for their ability to inhibit Ca^{2+} mobilization. Collectively, these studies indicate that BTP2 and its relatives provide a solid molecular framework for a new generation of small molecule inhibitors for the treatment of bronchial asthma, allergies, and other mast-cell mediated diseases.

Supplementary Material

Refer to Web version on PubMed Central for supplementary material.

Acknowledgments

We thank members of the August lab and the CMIID for feedback and discussion. We also thank E. Kunze, N. Bem and S. Magargee in the Center for Quantitative Cell Analysis at Penn State. This work was supported in part by grants from the NIH (AI51626, AI065566 & AI073955) to AA, CA83831 to BRP, and by the College of Agricultural Sciences at Penn State (to AA).

References

Baba Y, Nishida K, Fujii Y, Hirano T, Hikida M, Kurosaki T. Essential function for the calcium sensor STIM1 in mast cell activation and anaphylactic responses. Nat Immunol. 2008; 9:81–88. [PubMed: 18059272]

Bert A, Johnson B, Baxter E, Cockerill P. A modular enhancer is differentially regulated by GATA and NFAT elements that direct different tissue-specific patterns of nucleosome positioning and inducible chromatin remodeling. Mol Cell Biol. 2007; 27:2870–2885. Epub 2007 Feb 2875. [PubMed: 17283044]

Braun FJ, Aziz O, Putney JW Jr. 2-aminoethoxydiphenyl borane activates a novel calcium-permeable cation channel. Mol Pharmacol. 2003; 63:1304–1311. [PubMed: 12761340]

Chung SC, McDonald TV, Gardner P. Inhibition by SK&F 96365 of Ca2+ current, IL-2 production and activation in T lymphocytes. Br J Pharmacol. 1994; 113:861–868. [PubMed: 7858878]

De Boer M, Mordvinov V, Thomas M, Sanderson C. Role of nuclear factor of activated T cells (NFAT) in the expression of interleukin-5 and other cytokines involved in the regulation of hemopoetic cells. Int J Biochem Cell Biol. 1999; 31:1221–1236. [PubMed: 10582349]

Demo SD, Masuda E, Rossi AB, Throndset BT, Gerard AL, Chan EH, Armstrong RJ, Fox BP, Lorens JB, Payan DG, Scheller RH, Fisher JM. Quantitative measurement of mast cell degranulation using a novel flow cytometric annexin-V binding assay. Cytometry. 1999; 36:340–348. [PubMed: 10404150]

Di Capite J, Parekh AB. CRAC channels and Ca2+ signaling in mast cells. Immunol Rev. 2009; 231:45–58. [PubMed: 19754889]

Djuric SW, BaMaung NY, Basha A, Liu H, Luly JR, Madar DJ, Sciotti RJ, Tu NP, Wagenaar FL, Wiedeman PE, Zhou X, Ballaron S, Bauch J, Chen YW, Chiou XG, Fey T, Gauvin D, Gubbins E, Hsieh GC, Marsh KC, Mollison KW, Pong M, Shaughnessy TK, Sheets MP, Smith M, Trevillyan JM, Warrior U, Wegner CD, Carter GW. 3,5-Bis(trifluoromethyl)pyrazoles: a novel class of NFAT transcription factor regulator. J Med Chem. 2000; 43:2975–2981. [PubMed: 10956206]

Feske S. Calcium signalling in lymphocyte activation and disease. Nat Rev Immunol. 2007; 7:690–702. [PubMed: 17703229]

Franzius D, Hoth M, Penner R. Non-specific effects of calcium entry antagonists in mast cells. Pflugers Arch. 1994; 428:433–438. [PubMed: 7838664]

Gertler R, Pecht I. Ionic signalling in mast cells; antigen and ionophore induced changes in cytosolic pH. Mol Immunol. 1988; 25:1087–1092. [PubMed: 3221880]

Gessner A, Mohrs K, Mohrs M. Mast Cells, Basophils, and Eosinophils Acquire Constitutive IL-4 and IL-13 Transcripts during Lineage Differentiation That Are Sufficient for Rapid Cytokine Production. J Immunol. 2005; 174:1063–1072. [PubMed: 15634931]

Gomperts B, Cockcroft S, Bennett J, CM. F. Early events in the activation of Ca2+ dependent secretion: studies with rat peritoneal mast cells. J Physiol (Paris). 1980; 76:383–393. [PubMed: 6161245]

Gwack Y, Feske S, Srikanth S, Hogan P, Rao A. Signalling to transcription: store-operated Ca2+ entry and NFAT activation in lymphocytes. Cell Calcium. 2007; 42:145–156. [PubMed: 17572487]

Ishikawa J, Ohga K, Yoshino T, Takezawa R, Ichikawa A, Kubota H, Yamada T. A pyrazole derivative, YM-58483, potently inhibits store-operated sustained Ca2+ influx and IL-2 production in T lymphocytes. J Immunol. 2003a; 170:4441–4449. [PubMed: 12707319]

Ishikawa J, Ohga K, Yoshino T, Takezawa R, Ichikawa A, Kubota H, Yamada T. A pyrazole derivative, YM-58483, potently inhibits store-operated sustained Ca2+ influx and IL-2 production in T lymphocytes. J Immunol. 2003b; 170:4441–4449. [PubMed: 12707319]

Iyer A, August A. The Tec family kinase, IL-2-inducible T cell kinase, differentially controls mast cell responses. J Immunol. 2008; 180:7869–7877. [PubMed: 18523250]

Kiyonaka S, Kato K, Nishida M, Mio K, Numaga T, Sawaguchi Y, Yoshida T, Wakamori M, Mori E, Numata T, Ishii M, Takemoto H, Ojida A, Watanabe K, Uemura A, Kurose H, Morii T, Kobayashi T, Sato Y, Sato C, Hamachi I, Mori Y. Selective and direct inhibition of TRPC3 channels underlies biological activities of a pyrazole compound. Proc Natl Acad Sci U S A. 2009; 106:5400–5405. [PubMed: 19289841]

Klein M, Klein-Hessling S, Palmetshofer A, Serfling E, Tertilt C, Bopp T, Heib V, Becker M, Taube C, Schild H, Schmitt E, Stassen M. Specific and redundant roles for NFAT transcription factors in the expression of mast cell-derived cytokines. J Immunol. 2006; 177:6667–6674. [PubMed: 17082579]

Ma HT, Venkatachalam K, Parys JB, Gill DL. Modification of store-operated channel coupling and inositol trisphosphate receptor function by 2-aminoethoxydiphenyl borate in DT40 lymphocytes. J Biol Chem. 2002; 277:6915–6922. [PubMed: 11741932]

Melicoff E, Sansores-Garcia L, Gomez A, Moreira DC, Datta P, Thakur P, Petrova Y, Siddiqi T, Murthy JN, Dickey BF, Heidelberger R, Adachi R. Synaptotagmin-2 controls regulated exocytosis but not other secretory responses of mast cells. J Biol Chem. 2009; 284:19445–19451. [PubMed: 19473977]

Mercer J, Qi Q, Mottram L, Law M, Bruce D, Iyer A, Morales J, Yamazaki H, Shirao T, Peterson B, August A. Chemico-genetic identification of drebrin as a regulator of calcium responses. Int J Biochem Cell Biol. 2010; 42:337–345. Epub 2009 Dec 2003. [PubMed: 19948240]

Mercer JC, Qi Q, Mottram LF, Law M, Bruce D, Iyer A, Morales JL, Yamazaki H, Shirao T, Peterson BR, August A. Chemico-genetic identification of drebrin as a regulator of calcium responses. Int J Biochem Cell Biol. 42:337–345. [PubMed: 19948240]

Monticelli S, Lee D, Nardone J, Bolton D, Rao A. Chromatin-based regulation of cytokine transcription in Th2 cells and mast cells. Int Immunol. 2005; 17:1513–1524. [PubMed: 16199489]

Monticelli S, Solymar D, Rao A. Role of NFAT proteins in IL13 gene transcription in mast cells. J Biol Chem. 2004; 279:36210–36218. [PubMed: 15229217]

Ohga K, Takezawa R, Yoshino T, Yamada T, Shimizu Y, Ishikawa J. The suppressive effects of YM-58483/BTP-2, a store-operated Ca2+ entry blocker, on inflammatory mediator release in vitro and airway responses in vivo. Pulm Pharmacol Ther. 2008; 21:360–369. [PubMed: 17977764]

Peppiatt CM, Collins TJ, Mackenzie L, Conway SJ, Holmes AB, Bootman MD, Berridge MJ, Seo JT, Roderick HL. 2-Aminoethoxydiphenyl borate (2-APB) antagonises inositol 1,4,5-trisphosphate-induced calcium release, inhibits calcium pumps and has a use-dependent and slowly reversible action on store-operated calcium entry channels. Cell Calcium. 2003; 34:97–108. [PubMed: 12767897]

Plaut M, Pierce J, Watson C, Hanley-Hyde J, Nordan R, Paul W. Mast cell lines produce lymphokines in response to cross-linkage of Fc epsilon RI or to calcium ionophores. Nature. 1989; 339:64–67. [PubMed: 2469965]

Prakriya M, Lewis RS. Potentiation and inhibition of Ca(2+) release-activated Ca(2+) channels by 2-aminoethyldiphenyl borate (2-APB) occurs independently of IP(3) receptors. J Physiol. 2001; 536:3–19. [PubMed: 11579153]

Savignac M, Mellström B, Naranjo J. Calcium-dependent transcription of cytokine genes in T lymphocytes. Pflugers Arch. 2007; 454:523–533. Epub 2007 Mar 2002. [PubMed: 17334777]

Scharenberg AM, Kinet JP. PtdIns-3,4,5-P3: a regulatory nexus between tyrosine kinases and sustained calcium signals. Cell. 1998; 94:5–8. [PubMed: 9674420]

Schindl R, Kahr H, Graz I, Groschner K, Romanin C. Store depletion-activated CaT1 currents in rat basophilic leukemia mast cells are inhibited by 2-aminoethoxydiphenyl borate. Evidence for a regulatory component that controls activation of both CaT1 and CRAC (Ca(2+) release-activated Ca(2+) channel) channels. J Biol Chem. 2002; 277:26950–26958. [PubMed: 12011062]

Solymar D, Agarwal S, Bassing C, Alt F, Rao A. A 3' enhancer in the IL-4 gene regulates cytokine production by Th2 cells and mast cells. Immunity. 2002; 17:41–50. [PubMed: 12150890]

Stone K, Prussin C, Metcalfe D. IgE, mast cells, basophils, and eosinophils. J Allergy Clin Immunol. 2010; 125(2 Suppl 2):S73–80. [PubMed: 20176269]

Stone KD, Prussin C, Metcalfe DD. IgE, mast cells, basophils, and eosinophils. J Allergy Clin Immunol. 125:S73–80. [PubMed: 20176269]

Trevillyan JM, Chiou XG, Chen YW, Ballaron SJ, Sheets MP, Smith ML, Wiedeman PE, Warrior U, Wilkins J, Gubbins EJ, Gagne GD, Fagerland J, Carter GW, Luly JR, Mollison KW, Djuric SW. Potent inhibition of NFAT activation and T cell cytokine production by novel low molecular weight pyrazole compounds. J Biol Chem. 2001; 276:48118–48126. [PubMed: 11592964]

Turner H, Kinet JP. Signalling through the high-affinity IgE receptor Fc epsilonRI. Nature. 1999; 402:B24–30. [PubMed: 10586892]

Vig M, DeHaven WI, Bird GS, Billingsley JM, Wang H, Rao PE, Hutchings AB, Jouvin MH, Putney JW, Kinet JP. Defective mast cell effector functions in mice lacking the CRACM1 pore subunit of store-operated calcium release-activated calcium channels. Nat Immunol. 2008; 9:89–96. [PubMed: 18059270]

Wu J, Kamimura N, Takeo T, Suga S, Wakui M, Maruyama T, Mikoshiba K. 2-Aminoethoxydiphenyl borate modulates kinetics of intracellular Ca(2+) signals mediated by inositol 1,4,5-trisphosphate-sensitive Ca(2+) stores in single pancreatic acinar cells of mouse. Mol Pharmacol. 2000; 58:1368–1374. [PubMed: 11093775]

Yoshino T, Ishikawa J, Ohga K, Morokata T, Takezawa R, Morio H, Okada Y, Honda K, Yamada T. YM-58483, a selective CRAC channel inhibitor, prevents antigen-induced airway eosinophilia and late phase asthmatic responses via Th2 cytokine inhibition in animal models. Eur J Pharmacol. 2007; 560:225–233. [PubMed: 17307161]

Zitt C, Strauss B, Schwarz EC, Spaeth N, Rast G, Hatzelmann A, Hoth M. Potent inhibition of Ca2+ release-activated Ca2+ channels and T-lymphocyte activation by the pyrazole derivative BTP2. J Biol Chem. 2004; 279:12427–12437. [PubMed: 14718545]

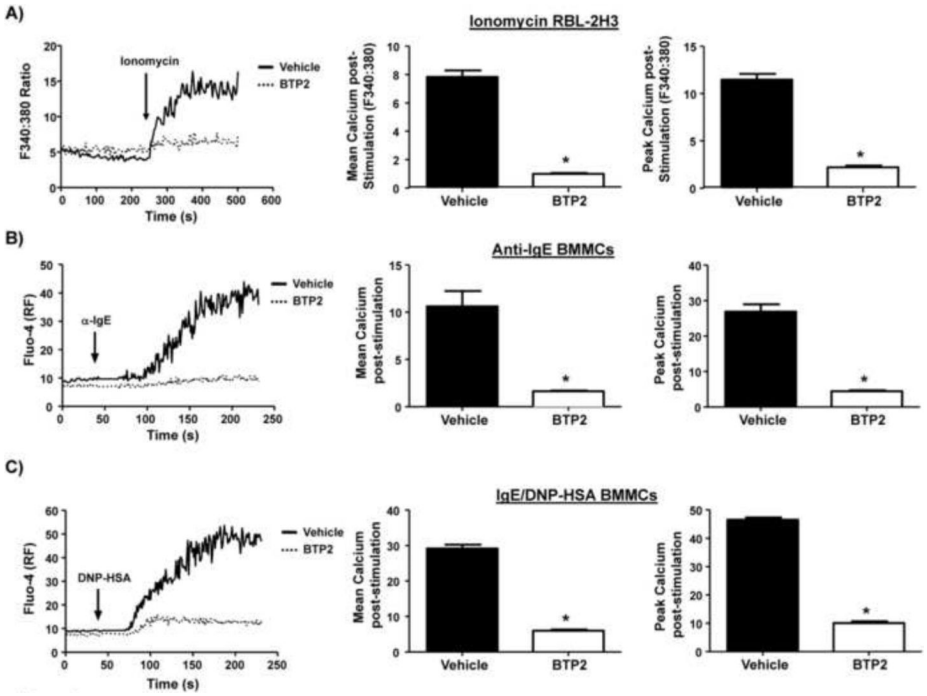

Figure 1. BTP2 blocks intracellular calcium mobilization in RBL-2H3 cells and BMMCs

(**A**) RBL-2H3 cells were pre-treated with BTP2 (1 μM) or vehicle (DMSO) for 30 min, then analyzed for calcium responses as described in the materials and methods following stimulation with 500 nM ionomycin in the presence of $CaCl_2$ for the indicated time period. $[Ca^{2+}]_i$ was expressed as ratiometric Fura-2AM, and representative data of 3–5 independent experiments is shown (left panel). Quantification of mean calcium increase (middle panel); peak calcium increase (right panel), with data expressed as the mean ± SEM of 3–5 independent experiments. *p<0.05 vs. Vehicle. (**B**) BMMCs were pre-treated with BTP2 (1 μM) or vehicle for 30 min, then stimulated with mouse anti-DNP IgE and rat anti-mouse IgE (10 μg/mL), and analyzed as in (A), except that $[Ca^{2+}]_i$ was expressed as Fluo-4 relative fluorescence with representative data of 3–5 independent experiments shown (left panel). Quantification of mean calcium increase (middle panel); peak calcium increase (right panel) as in (A). Data are expressed as the mean ± SEM of 3–5 independent experiments. *p<0.05 vs. Vehicle. (**C**) BMMCs were pre-treated with BTP2 (1 μM) or vehicle for 30 min, then stimulated with 100 ng DNP-HSA and analyzed as in (A), except that $[Ca^{2+}]_i$ was expressed as Fluo-4 relative fluorescence with representative data of 3–5 independent experiments shown (left panel). Quantification of mean calcium increase (middle panel); peak calcium increase (right panel) as in (A). Data are expressed as the mean ± SEM of 3–5 independent experiments. *p<0.05 vs. Vehicle.

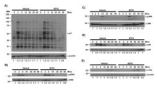

Figure 2. BTP2 does not affect tyrosine kinase nor MAP kinase activation following FcεRI triggering

BMMCs were treated with either BTP2 (1 μM) or vehicle (DMSO) for 30 min and then stimulated with mouse IgE anti-DNP and DNP-HSA for the indicated time periods, lysed, and analyzed by western blot for (**A**) total phosphotyrosine; (**B**) phospho-ERK; (**C**) phospho-JNK; (**D**) phospho-p38; or (**E**) c-Fos expression. Blots were stripped and reprobed with control antibodies for β-actin. Numbers indicate fold increase corrected for expression levels.

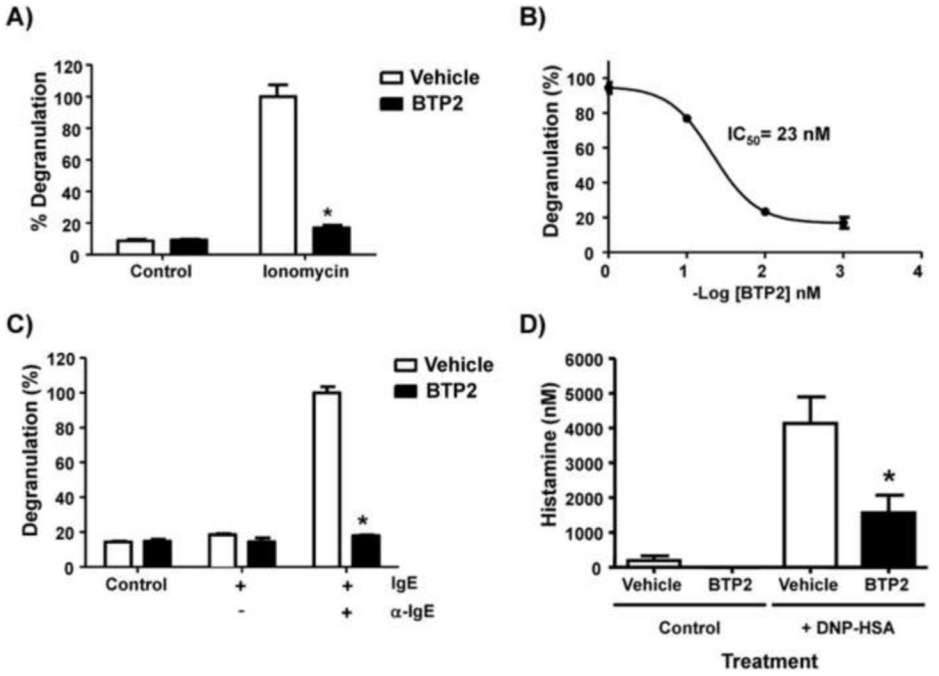

Figure 3. BTP2 inhibits mast cell degranulation *in vitro* and FcεRI-mediated histamine release *in vivo*

(**A**) RBL-2H3 cells were pretreated with BTP2 or vehicle (DMSO) at 1 μM and then stimulated with ionomycin (500 nM) for 30 minutes. (**B**) RBL-2H3 cells were pretreated with vehicle (DMSO) or BTP2 at the indicated concentrations for 30 minutes then stimulated as in (A). (**C**) RBL-2H3 cells were pretreated with BTP2 (1 μM) or vehicle for 30 min, then stimulated with mouse IgE anti-OVA and rat anti-mouse IgE for 30 min. All cells were analyzed for degranulation via an annexin-V binding assay. Data are expressed as the mean ± SEM of 3 independent experiments. *p<0.05 vs. Vehicle. **(D)** C57BL/6 mice were sensitized with mouse IgE anti-DNP overnight, then treated with BTP2 (BTP2, 10 mg/kg) or vehicle (DMSO) for 1 hour. Mice, treated with BTP2 or vehicle, were then challenged with DNP-HSA or PBS (as a control) for 3 min. Serum histamine concentration levels were then determined and data are expressed as the mean ± SEM, n=8 except for control mice treated with BTP and no antigen, n=3. *p<0.05 vs. Vehicle.

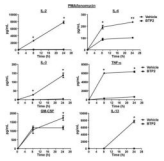

Figure 4. BTP2 inhibits cytokine secretion of PMA/ionomycin-activated BMMCs

BMMCs were pretreated with BTP2 (1 μM) or vehicle (DMSO) for 30 min, then stimulated with PMA and ionomycin. 8 and 24 hours after stimulation, the concentration of the indicated cytokines were determined. Data are expressed as the mean ± SEM of technical non-independent replicates, representative of 3 independent experiments. *$p<0.05$ vs. Vehicle.

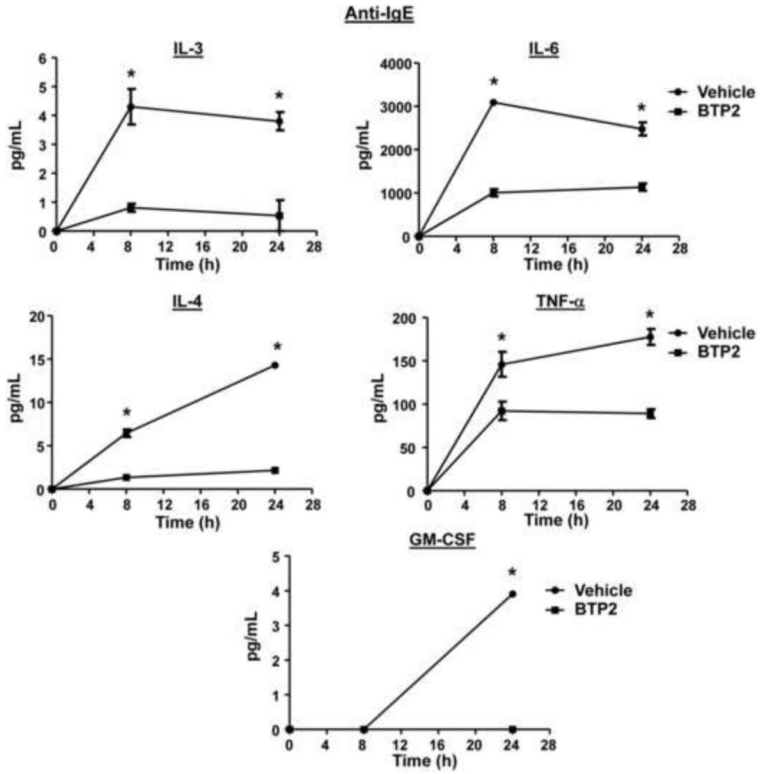

Figure 5. BTP2 inhibits cytokine secretion of IgE/anti-IgE-activated mast cells

BMMCs were sensitized with mouse anti-DNP IgE, pretreated with BTP2 (1 μM) or vehicle (DMSO) for 30 min, and then stimulated rat anti-mouse IgE. 8 and 24 hours after stimulation, the concentration of the indicated cytokines were determined. Data are expressed as the mean ± SEM of technical non-independent replicates, representative of 3 independent experiments. *$p<0.05$ vs. Vehicle.

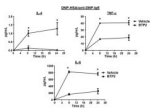

Figure 6. BTP2 inhibits cytokine secretion of IgE/antigen-mediated activation of mast cells

BMMCs were sensitized with mouse anti-DNP IgE, pretreated with BTP2 (1 μM) or vehicle (DMSO) for 30 min, and then stimulated with DNP-HSA (100 ng/mL). 8 and 24 hours after stimulation, the concentration of the indicated cytokines were determined. Data are expressed as the mean ± SEM of technical non-independent replicates, representative of 3 independent experiments. *p<0.05 vs. Vehicle.

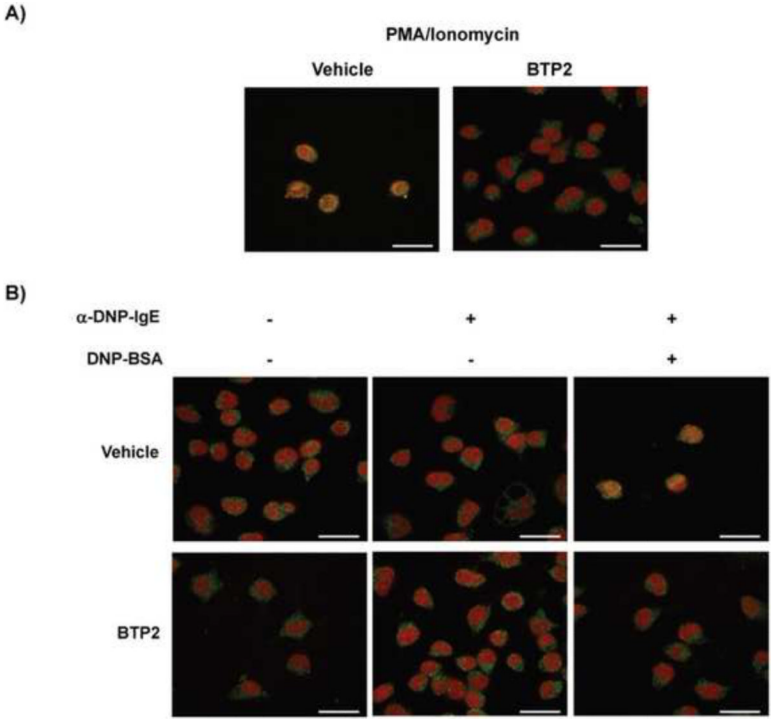

Figure 7. BTP2 inhibits stimulus-induced NFAT nuclear translocation

(**A**) RBL-2H3 cells were pretreated with BTP2 (1 μM) or vehicle (DMSO) for 30 min prior to stimulation for 45 min with ionomycin or (**B**) mouse anti-DNP IgE and DNP-HSA (100 ng/mL). Cells were fixed and permeabilized, and NFATc1 localization determined by confocal microscopy. The nucleus was identified using TO-PRO-3 staining, and nuclear localization of NFAT is evident by the yellow nuclear staining (red plus green). White bars indicate 40 μm. Representative data of 3–5 independent experiments is shown.

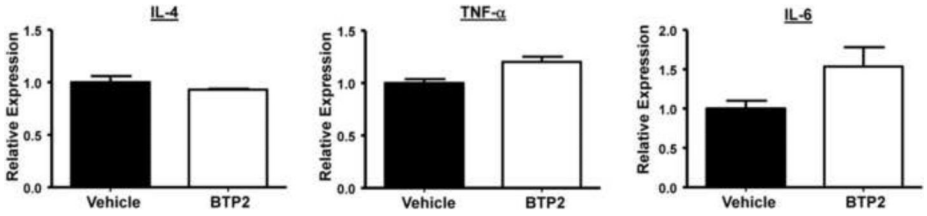

Figure 8. BTP2 does not affect preformed cytokine mRNA expression

BMMCs were pretreated with BTP2 (1 μM) or vehicle (DMSO) for 2 days and levels of IL-4, IL-6, and TNF-α were quantified. Data are expressed as the mean ± SEM of duplicate experiments.

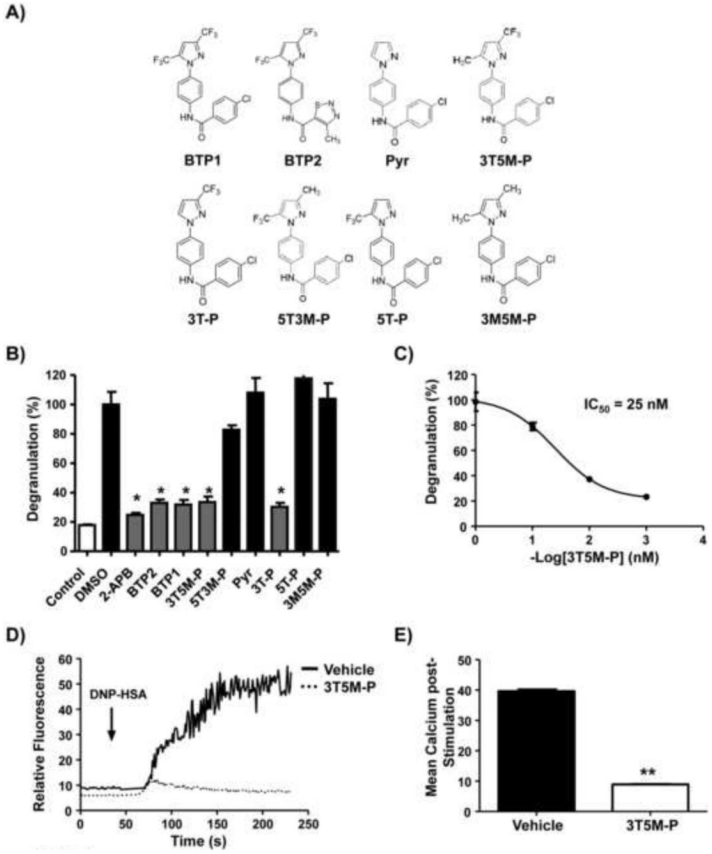

Figure 9. The 3-trifluoromethyl group is critical for BTP2 activity

(**A**) Structures of BTP2 and derivatives (BTP1; BTP2; Pyrazole: Pyr; 3-trifluoromethyl-5-methyl-pyrazole: 3T5M-P; 3-trifluoromethyl-pyrazole: 3T-P; 5-trifluoromethyl-3-methyl-pyrazole: 5T3MP; 5-trifluoromethyl-methyl-pyrazole: 5T-P; 3-methyl-5-methyl-pyrazole: 3M5M-P). (**B**) BMMCs were pretreated with vehicle, 2-APB (at 50 μM), or BTP analogs (at 1 μM) and then stimulated with ionomycin. Degranulation was determined as indicated in materials and methods. (**C**) RBL-2H3 cells were pretreated with vehicle or the indicated BTP analogs at 1 μM (left panel) or 3T5M-P at the indicated concentrations (right panel). Cells were then stimulated with ionomycin and degranulation determined as in figure 3. (**D**) BMMCs were pretreated with 3T5M-P (1 μM) or vehicle for 30 min, then stimulated with mouse IgE anti-DNP and DNP-HSA (100 ng/mL). Calcium responses were determined as in figure 1. Representative data of 3–6 experiments is shown. (**E**) Mean calcium increase. Data are expressed as the mean ± SEM of 3 independent experiments. Data are expressed as the mean ± SEM of 3 independent experiments. *,**$p < 0.05$ vs. vehicle.